ISSN 1392 - 1207. MECHANIKA. 2009. Nr.5(79)

Computation of turbulent channel flow with variable spacing riblets

M. E. Benhamza*, F. Belaid**
**LAIGM, Engineering Process Dept, 8 Mai 45, Guelma University, B.P. 401, 24000 Guelma, Algeria, E-mail: benhamza@hotmail.com*
***LAIGM, Engineering Process Dept, 8 Mai 45, Guelma University, B.P. 401, 24000 Guelma, Algeria, E-mail: bel_fair@yahoo.fr*

1. Introduction

Many applications in aerodynamic, hydrodynamic and in pipelines can be greatly benefited from any significant amount of drag reduction. Longitudinal microgrooves aligned in the flow direction known as riblets stand as the most convenient and practical techniques applied in real applications for drag reduction. Considerable studies have been devoted to the development of an optimum shape of riblets in order to improve the net drag reduction. Different shapes including the L, V, and U cross-sections have been investigated experimentally and numerically.

Initial experimental studies on riblets were conducted by Walsh [1, 2] at NASA Langley Research Center. They were devoted to optimize the riblet size and shape for a maximum drag reduction. Suzuki and Kasagi [3] used PTV for measuring the velocity field in near triangular riblet region while Park and Wallace [4] used hot-wires in their measurements. Both Choi [5] and Tang and Clark [6] examined the influence of L-shaped riblets on burst frequency using flow visualization and hot wire anemometry. Bechert et al. [7, 8] have investigated more thoroughly different configurations of riblets including rectangular, scalloped and shark-skin-shape riblets.

Analytical methods applied to calculate vibrations of ribbed plates are very complicated, therefore modeling is more convenient for the investigation [9].

Moreover, numerical methods such as direct numerical simulation (DNS) and Reynolds average Navier Stokes (RANS) have been applied to study the turbulent flow over riblets. Choi et al. [10] and Chu and Karniadakis [11] have performed DNS using the finite volume and the spectral element methods respectively for triangular riblets. Results of the DNS method are consistent, at least qualitatively; together with the available experimental data they have extended the knowledge of the turbulence structure over this complex surface. However, DNS which is relatively costly is still limited to low Reynolds number flows which are not representative of most of the real conditions. Thus, RANS approach remains an alternative.

Launder and Li [12,13] and Djenidi et al. [14-16] have used two-equation turbulence model. Their results showed less agreement with experimental data and the difficulty in predicting correctly the drag variation when adopting isotropic models [17]. In contrary, Benhalilou et al. [18] used a nonlinear two-equation model to investigate heat and momentum transfer characteristic. Their results show that the drag reduction and secondary motion have been accurately predicted due to the anisotropic model considered. Recently, Horsten [19] and El-Sameni et al. [20] have adopted successfully an IBM for V and L-shaped riblets aiming at underlying the form and the thickness effect of the riblets's tip.

In the present research study, a new riblet configuration which has not been tested before is suggested; retaining the riblet structural simplicity but trying to improve its drag reduction performance. For this purpose, different L shaped blades' structure have been examined, i.e. a progressive with increasing spacing, a regressive with decreasing spacing and for comparison a uniform spacing. In order to maintain the identical flow conditions, the same wetted area of the blade surfaces is considered for all the cases. Turbulent incompressible flow modeling in a rectangular duct with the proposed blade wall is considered in this study. Reynolds stress model (RSM) is used to describe the fluid behavior over these riblets. Unlike the other method cited above, RSM approach consists in solving the individual Reynolds stresses, using differential transport equations. The individual Reynolds stresses are then used to obtain closure of the Reynolds-averaged momentum equation. This method is chosen because it gives the best results in predicting such complex flows, especially when the flow features of interest are the result of anisotropy in Reynolds stresses.

2. Numerical simulation

With the assumption of incompressible turbulent flow, the RANS equations can be written in Cartesian coordinates as

$$\frac{\partial \overline{u}_i}{\partial x_i} = 0 \tag{1}$$

$$\frac{\partial \overline{u}_i}{\partial t} + \frac{\partial (\overline{u}_i \overline{u}_j)}{\partial x_j} = -\frac{1}{\rho}\frac{\partial \overline{p}}{\partial x_i} + \frac{\partial}{\partial x_j}\left[\nu\left(\frac{\partial \overline{u}_i}{\partial x_j} + \frac{\partial \overline{u}_j}{\partial x_i} - \frac{2}{3}\frac{\partial \overline{u}_i}{\partial x_i}\delta_{ij}\right) - \tau_{ij}\right] \tag{2}$$

where $\overline{u}_i$ is the mean velocity components ($i = 1, 2, 3$), p is the pressure, ρ is the fluid density, ν is the kinematic viscosity and δ is the Kronecker delta. These equations contain additional terms τ_{ij} which are the Reynolds stresses representing the effects of turbulence defined as

$$\tau_{ij} = \overline{u_i' u_j'} \tag{3}$$

with u_i' the fluctuating velocity component.

To close the RANS equation, RSM is adopted to solve transport equations for the Reynolds stresses, to-

gether with an equation for the dissipation rate. The exact transport equations of the Reynolds stresses may be written as follows

$$\frac{\partial \tau_{ij}}{\partial t} + C_{ij} = D_{T,ij} + D_{L,ij} + P_{ij} + \phi_{ij} + \varepsilon_{ij} \tag{4}$$

with

- $C_{ij} = \frac{\partial}{\partial x_k}\left(\rho u_k \tau_{ij}\right)$ the convection term;
- $D_{L,ij} = \frac{\partial}{\partial x_k}\left(\nu \frac{\partial \tau_{ij}}{\partial x_k}\right)$ the molecular diffusion term;
- $P_{ij} = -\left(\tau_{ik}\frac{\partial u_j}{\partial x_k} + \tau_{jk}\frac{\partial u_i}{\partial x_k}\right)$ the production term, do not require any modeling.

However, the remaining ones need to be modeled to close the equations, which are:

- the turbulent diffusion,
- $D_{T,ij} = -\frac{\partial}{\partial_{xk}}\left[\overline{u_i' u_j' u'}_k + \overline{\frac{p}{\rho}\left(\delta_{kj}u_i' + \delta_{ik}u'j\right)}\right]$
- the pressure strain, $\phi_{ij} = \overline{\frac{p}{\rho}\left(\frac{\partial u_i'}{\partial x_j} + \frac{\partial u_j'}{\partial x_i}\right)}$
- the dissipation, $\varepsilon_{ij} = -2\nu\overline{\frac{\partial u_i'}{\partial x_k}\frac{\partial u_j'}{\partial x_k}}$.

More information to describe the modeling assumptions required to close the equation set could be found in Fluent [21].

3. Computational details

The flow geometry and coordinate system are shown in Fig. 1. The upper wall is a flat plate, whereas the lower wall is a ribbed plate. Fully developed turbulent flow over riblets is considered homogeneous in the streamwise (x) direction, so periodic boundary condition is used in that direction. The nonslip condition is applied for all walls. Only half of the channel is simulated to minimize the computational loading, and a symmetry condition is used at the plane z = 0. A constant instantaneous volume flux is imposed in the streamwise direction as:

$$Q = \int_A u dA = \frac{2}{3} A_c U_c \tag{5}$$

where U_c is the cross-sectional area, and A_c is the centerline velocity of a laminar parabolic profile with the same volume flux. The computation is carried out for a constant Reynolds number $Re = U_c \delta / \nu$ of 4200, δ is the half width of the channel.

The computational domain has the dimensions 3δ, 2δ and δ in x, y and z direction respectively which is sufficient to carry the amount of turbulent flow conditions. It is relatively one and half larger than the minimal flow unit as estimated by Jimenez and Moin [22] for turbulent channel flow.

The cross-section of the blades is depicted in Fig. 2. Due to various geometrical parameters of riblets used here, the spacing to height ratio s/h is fixed at 1 and the thickness to height ratio t/h is set to 0.04, when considering uniform spacing blades. But when considering regressive and progressive spacing blades only s is variable, and the obtained spacing to height ratios are within $0.5 \le s/h \le 1.5$. The wetted area of the blade surfaces does not vary in the three cases. The chosen dimensions' ratio are as reported in other studies.

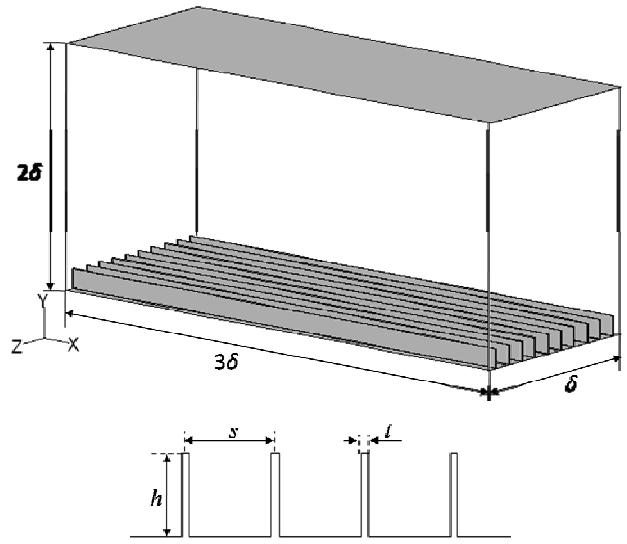

Fig. 1 Computational domain

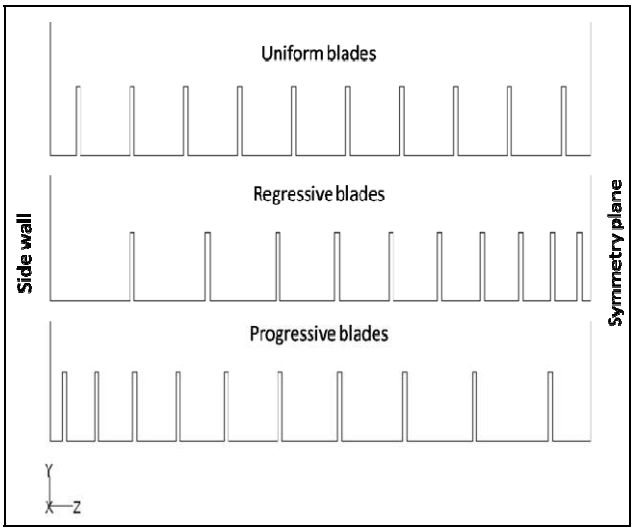

Fig. 2 Representation of the three blades cases on the channel cross-section

4. Results and discussions

4.1. Velocity field

The mean velocity profiles in wall units shown in Fig. 3 are in excellent matching with the wall laws method. In general, the velocity values near the wall decrease significantly above the ribbed surface. A little shift up of the velocity profile is observed from the RSM calculation compared to the linear law of the wall. When considering the velocity profile within the valley, it can be noted that the variation of the streamwise velocity gradient strongly depends on riblet's spacing, as can be seen in Fig. 4. The

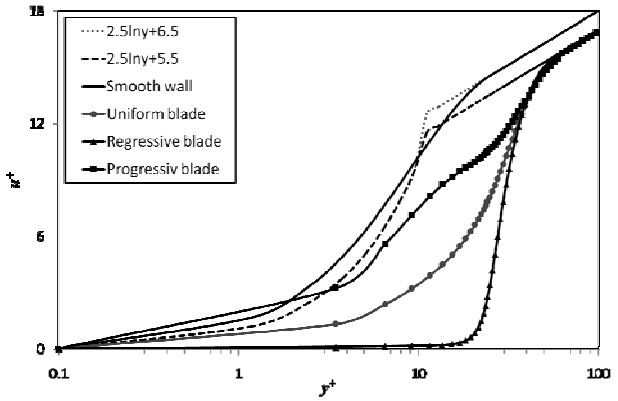

Fig. 3 Variation of mean velocity profiles normalized by the wall units in comparison with laws of the wall, (the wall coordinate: $u^+ = u/u_t$, where u_t is the friction velocity and $y^+ = yu_t/\nu$)

contribution of velocity gradient on the total friction drag is significant due to the large area of the blade valley and very steep velocity gradients occur around the tip of the riblets. All profiles plotted over the riblets' tips and valleys overlap further away from the buffer layer, which indicate that riblets does not affect the outer flow region.

4.2. Drag reduction

The optimum value of riblet spacing obtained in the present calculation at which the drag reduction would be a maximum is in accordance with previous studies of different riblets. The drag variation ratio is defined as

$$Dr = \left(Cf_r - Cf_s\right)/Cf_s \tag{6}$$

where Cf_r and Cf_s are the skin friction coefficient at the ribbed wall and the corresponding smooth wall. The ob-

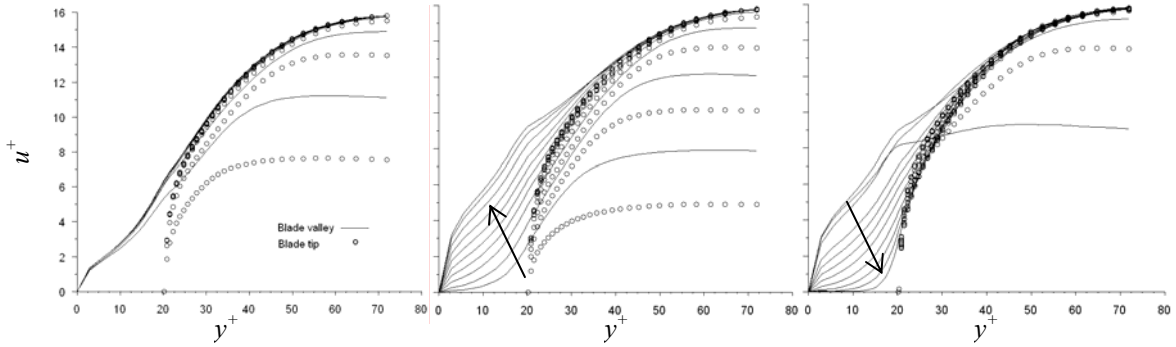

Fig. 4 Mean velocity profiles normalized by the wall units at different spanwise positions: a - uniform spacing blade; b - progressive spacing blade; c - regressive spacing blade. Up and down arrows shows spanwise direction from the side to symmetry plane

Table
Dimensionless spacing and drag reduction variation ratio in percent

Blade spacing	s^+	Dr, %	
		Data from [19]	Present calculation
Uniform	20	12	12.29
Regressive	12 – 36		12.43
Progressive			11.67

tained results compared to experimental and DNS results for similar nondimensional spacing s^+, which are summarized in Table, show a reasonable agreement.

4.3. Turbulence intensities

The magnitude of root mean square (RMS) of streamwise velocity fluctuations averaged by the mean velocity is shown in Fig. 5. Results of turbulent intensity in cross flow plane show that significant variations occur only in the vicinity of the wall [9]. The general trend of the streamwise component u_{rms} near riblet region is reduced compared to smooth surface values. The maximum magnitude u_{rms} of is reduced by 13.72% above the blade, this is in fact close to the experimental results obtained by Walsh (where reduction is of 16%) and DNS results of Choi [9] (where reduction is of 12%). The reduction within the grooves is larger for regressive spacing blade; this is due to the reduction of flow's dynamic activity. Thus, these results indicate the reliability of the present approach to produce accurate second-order statistics.

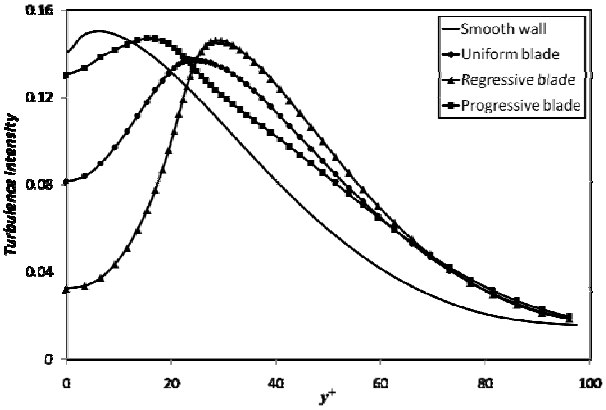

Fig. 5 Turbulence intensity profiles in global units at the symmetric plane

4.4. Reynolds shear stresses

The Reynolds shear stresses are plotted in Fig. 6 for the three blades' configurations, in which the stress is suppressed especially for the minimum blade spacing due

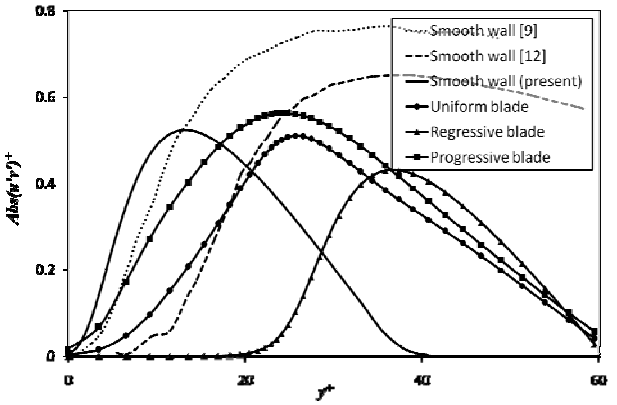

Fig. 6 Reynolds shear stress in wall units at the symmetric plane

to attenuation of the near-wall activities. This suggests again turbulent activities in that layer have been much suppressed. The peaks of curves are in different position and shifted up at higher y^+. The distance between the peak of $\overline{u'v'}$ profile on the ribbed surface and that of the smoothone is around 10 to 20 wall units. Fig. 7 presents Reynolds shear stress contours plot above the blade valleys and tips where it can be shown that shear stresses near the wall depend for most on the blade spacing.

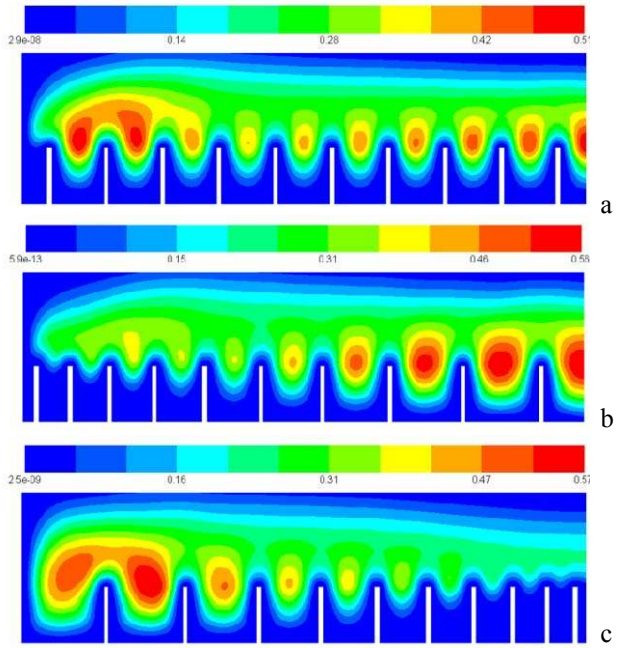

Fig. 7 Contour plots of Reynolds shear stresses on cross plane ($y^+ = 60$): a - uniform blade; b - progressive blade; c - regressive blade

4.5. Flow structures

It is known that near the smooth wall, the ejection and sweep events occur especially in the corner of the channel. Few snap shots and contours are presented to support the above mentioned observations. Fig. 8 shows the streamwise velocity contours embedded with the cross flow velocity vectors v and w obtained on a periodic plane, where large secondary motion can be observed outward the riblets. This enclosed larger eddies found above riblets tip, block the high speed fluid far

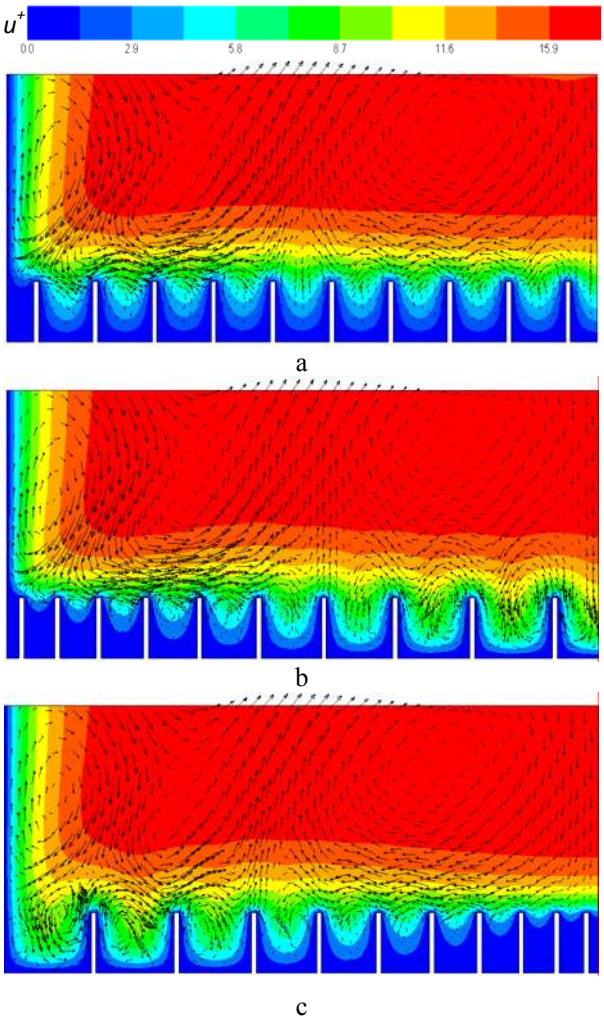

Fig. 8 Cross streamwise velocity contours embedded with secondary velocity vectors: a - uniform spacing blade; b - progressive spacing blade; c - regressive spacing blade

away from the wall. Such set-up results are in a damped zone of h thickness with insignificant activities; this indicates that the riblets have moved the near-wall activities and their evolving turbulent structures mostly away from the wall. This setting of turbulent eddies supports the idea of getting a damping layer when the riblet spacing becomes narrower enough to prevent the penetration and residence of vortical structures into the riblets valleys.

5. Conclusion

From this calculation study, it is shown that secondary flows are easily introduced inside the valleys of broad spacing thus exposing a greater surface to the movement of sweeping. However, the grooves of less spacing block this recirculation outside the grooves and consequently the wet surface is prone to weak movement.

Despite the same blade wetted area of all cases, the regressive spacing blade has revealed an increase of about 1.14% in drag reduction efficiency compared to progressive one. The setting of turbulent eddies supports the idea of getting a damping layer when the blade spacing becomes narrower enough in the core of the channel, to prevent the penetration and residence of vortical struc-

tures into the riblets valleys.

Generally, RSM is a appropriate to predict accurately drag reduction and velocity profile, though large discrepancies were found in the Reynolds stress values. The magnitude of the Reynolds stress is severely underpredicted, in particular within the core of the channel.

The main result of the paper confirms that all riblets or microstructures' spacing should always be narrower in the flow core, such as found in zoological observations.

References

1. **Walsh**, **M.J.** Turbulent boundary layer drag reduction using Riblets.-AIAA paper, 1982, 82, p.0169.
2. **Walsh**, **M.J.** Riblet/LEBU research at NASA Langley. -Applied Scientific Research, 1989, 46, p.255-262.
3. **Suzuki, Y., Kasagi, N.** Turbulent drag reduction mechanism above a riblet surface.-AIAA Journal, 1994, 32(9), p.1781-1790.
4. **Park, S.-R., Wallace**, **J.M.** Flow alteration and drag reduction by riblets in a turbulent boundary layer. -AIAA Journal, 1994, 32, p.31-38.
5. **Choi**, **K.S.** Near-wall structure of turbulent boundary layer with riblets. -Journal of Fluid Mechanics, 1989, 208, p.417-458.
6. **Tang, Y.P., Clark**, **D.G.** On near-wall turbulence generating events in a turbulent boundary layer on a riblet surface. -Applied Scientific Research, 1993, 50, p.215-232,
7. **Bechert, D.W., Bruse, M., Hage**, **W.** Experiments with three-dimensional riblets as an idealized model of shark skin.-Experiments in Fluids, 2000, 28, p.403-412.
8. **Bechert, D.W., Hoppe, G., Van der Hoeven, J.G., Makris**, **R.** The Berlin oil channel for drag reduction research. -Experiments in Fluids, 1992, p.251-260.
9. **Setkauskas, V., Vyšniauskienė, Ž.** Investigation of ribbed plate vibrations in viscous fluid. -Mechanika. -Kaunas: Technologija, 2002, Nr.3(35), p.34-37.
10. **Choi, H., Moin, P., Kim, J.** Direct numerical simulation of turbulent flow over riblets. -Journal of Fluid Mechanics, 1993, 255, p.503-539.
11. **Chu, D.C., Karniadakis**, **G.E.** A direct numerical simulation of laminar and turbulent flow over riblet-mounted surfaces.-Journal of Fluid Mechanics, 1993, 250, p.1-42.
12. **Launder, B.E., Li**, **S.P.** A numerical study of riblet effects on laminar flow through a plane channel. -Applied Scientific Research, 1989, 46, p.271-279.
13. **Launder, B.E., Li, S.P.** On the prediction of riblet performance with engineering turbulence models. -Applied Scientific Research, 1993, 50, p.283-298.
14. **Djenidi, L., Antonia, R.A.** Riblet modelling using a second-moment closure.-Applied Scientific Research, 1995, 54, p.249-266.
15. **Djenidi, L., Antonia, R.A.** Riblet flow calculation with a low Reynolds number k - epsilon model. -Applied Scientific Research, 1993, 50, p.267-282.
16. **Djenidi, L., Liandrat, J., Anselmet, F., Fulachier**, **L.** Numerical and experimental investigation of the laminar boundary layer over riblets. -Applied Scientific Research, 1989, 46, p.263-270.
17. **Benhalilou, M., Kasagi**, **N.** Numerical prediction of heat and momentum transfer over micro-grooved surface with a nonlinear k-e model.-International Journal of Heat and Mass Transfer, 1999, 42, p.1414-1430.
18. **Coustols**, **E.** Effet des parois rainurées ("riblets") sur la structure d'une couche limite turbulente. -Mécanique Industrielle, 2001, p.421-434.
19. **Horsten, B.J.** A numerical study on laminar and turbulent flow over sharp and blunt sawtooth riblets. Viscous drag reduction mechanisms reviewed.-Delft, 2005.
20. **El-Samni, H.H. Chun, H.S. Yoon**, Drag reduction of turbulent flow over thin rectangular riblets.-International Journal of Engineering Science, 2007, 45, p.436-454.
21. Fluent Inc., Fluent 6.3 documentation, 10 Cavendish Court, Lebanon, NH 03766, USA, 2006.
22. **Jimenez, J., Moin, P.** The minimal flow unit in near wall turbulence. -Journal of Fluid Mechanics, 1999, 225, p.213-240.

M. E. Benhamza, F. Belaid

TURBULENCINIO TEKĖJIMO KANALE SU KINTAMU ATSTUMU IŠDĖSTYTOMIS BRIAUNOMIS SKAIČIAVIMAS

R e z i u m ė

Žinoma, kad išilginės briaunos, suformuotos plokščiame paviršiuje, sumažina turbulencinį plėvelės pasipriešinimą trinčiai, todėl ją vidutiniškai galima sumažinti nuo 4 iki 8 %. Šiame straipsnyje tyrinėjamos nestandartinės briaunos, išdėstytos kintamu atstumu. Jos panaudotos vietoj vienodu atstumu išdėstytų griovelių. Skaitinis turbulencinio tekėjimo briaunomis padengtu paviršiumi modeliavimas atliktas trimis atvejais: esant pastoviam, didėjančiam ir mažėjančiam atstumui tarp briaunų. Visos briaunos yra stačiakampės formos, kaip ir drėkinamoji sritis. Gauti rezultatai rodo, kad pasipriešinimo sumažėjimas labai priklauso nuo atstumo tarp briaunų pokyčio. Jis gerėja esant regresyviam (pamažu mažėjančiam) tarpo kitimui. Priešingos tendencijos pastebimos esant progresyviam (pamažu didėjančiam) tarpo kitimui.

Skirtingas tekėjimo pobūdis trimis briaunoto paviršiaus atvejais nustatytas stebint tekėjimą skersiniame pjūvyje, kitaip dar vadinamą skersinio srauto greičiu arba Reinoldso įtempiais. Tyrimais nustatyta, kad skersinio tekėjimo turbulencijos intensyvumas mažėja esant regresyviam briaunų išdėstymui, palyginti su progresyviu ir pastoviu briaunų išdėstymu.

M. E. Benhamza, F. Belaid

COMPUTATION OF TURBULENT CHANNEL FLOW WITH VARIABLE SPACING RIBLETS

S u m m a r y

It is known that longitudinal ribs manufactured

in a flat surface act to reduce (reduces) turbulent skin-friction drag, thus providing a moderate drag reduction of 4 to 8%. In this paper, nonconventional variable blades are used instead of uniform grooves. Numerical simulation of a turbulent flow over blade-covered surface is performed for three cases: uniform, increasing and decreasing spacing blades. All riblets have rectangular cross-section as well as the same wetted area. Results show that drag reduction is strongly depending on the spacing variation, showing a benefit over uniform riblets for regressive spacing, and an opposite trend for the progressive one.

Different nature of the flow over the three cases of blades' surfaces is revealed by looking at transverse planes cross flow motion, mean streamwise velocity and Reynolds stresses. Results show cross flow turbulence intensity reduced for regressive riblets compared to progressive and uniform ones.

М. Э. Бенгамза, Ф. Белаид

ВЫЧИСЛЕНИЕ ТУРБУЛЕНТНОГО ПОТОКА В КАНАЛЕ С ИЗМЕНЯЮЩИМСЯ РАССТОЯНИЕМ МЕЖДУ НАПРАВЛЯЮЩИМИ РЕБРАМИ

Р е з ю м е

Известно, что продольные ребра, сформированные на плоской поверхности, уменьшают турбулентное сопротивление пленки к трению (к течению) в среднем от 4 до 8%. В статье исследуется применение нестандартных ребер, расположенных в канале с переменным расстоянием между ними. Они использованы взамен равномерных канавок. Численное моделирование турбулентного течения по каналу с ребрами произведено для трех случаев: при равномерном, увеличивающимся и уменьшающимся расстояниями между ребрами. Все ребра в поперечном сечении имеют прямоугольную форму, как и оросительная часть канавки. Полученные результаты показывают, что сопротивление сильно зависит от изменения расстояния между ребрами. Оно уменьшается при регрессивном изменении расстояния между ребрами. Противоположные тенденции проявляются при прогрессивном изменении расстояния.

Различная природа течения потока при трех случаях определения наблюдением течения потока в поперечном сечении, которое еще называют скоростью поперечного потока или напряжением Рейнольдса. Исследованиями установлено, что интенсивность турбулентности поперечного течения потока уменьшается при наличии регрессивного расположения ребер по сравнению с прогрессивным и постоянным расположением ребер.

Received June 05, 2009
Accepted October 12, 2009